Available online at www.sciencedirect.com

ScienceDirect

Procedia Structural Integrity 3 (2017) 217–223

Structural Integrity Procedia

www.elsevier.com/locate/procedia

XXIV Italian Group of Fracture Conference, 1-3 March 2017, Urbino, Italy

Crack path and damage in a CuZnAl SMA

V. Di Cocco[a,*], F. Iacoviello[a], L. D'Agostino[a], S. Natali[b], V. Volpe[b]

[a]*Università di Cassino e del Lazio Meridionale, DICeM, via G. Di Biasio 43, 03043 Cassino (FR), Italy*
[b]*Università di Roma "La Sapienza", DICMA, via Eudossiana 18, 00184, Roma, Italy*

Abstract

Pseudo-elastic (PE) materials are an important class of metallic alloy which exhibit unique features with respect to common engineering metals. In particular, due to these properties PEs are able to recover their original shape after high values of mechanical deformations, by removing the mechanical load (PE). From the microstructural point of view shape memory and pseudo-elastic effects are due to a reversible solid state microstructural diffusionless transitions from austenite to martensite, which can be activated by mechanical and/or thermal loads. Copper-based shape memory alloys are preferred for their good memory properties and low cost of production.
In this work the main crack initiation and its propagation in a tensile test is analyzed in order to evaluate crack path and its behavior at low and at high values of deformation. Results are also associated both to grains boundary chemical properties and to X-ray diffraction, in order to correlate structural transition involved in an Cu-Zn-Al alloy characterized by a PE behavior.

Keywords: Zn-Cu-Al alloy; Pseudoeleastic behaviour; Crack micromechanisms.

1. Introduction

Shape memory alloys (SMA) and pseudo-elastic alloys (PEA) are able to recover their original shape after high mechanical deformations: the first ones by heating up to characteristic temperature (Shape Memory Effect, SME), and the second ones simply by removing the mechanical load (Pseudo-elastic Effect, PE).

* Corresponding author. Tel.: +39.07762994334.
E-mail address: v.dicocco@unicas.it

10.1016/j.prostr.2017.04.049

Nomenclature

LVDT	Linear Variable Differential Transformer
SEM	Scanning Electron Microscope
XRD	X Ray Diffraction

Different shape memory alloys have been optimized in the last decades, such as the copper-zinc-aluminum (ZnCuAl), copper-aluminum-nickel (CuAlNi), nickel-manganese-gallium (NiMnGa), nickel-titanium (NiTi), and other SMAs obtained alloying zinc, copper, gold, iron, etc.. However, the near equiatomic NiTi binary system shows the most interesting properties and it is currently used in an increasing number of applications in many fields of engineering, for the realization of smart sensors and actuators, joining devices, hydraulic and pneumatic valves, release/separation systems, consumer applications and commercial gadgets as Otsuka et all. (2005) and Dong. et all. (2008). Due to their good biocompatibility, another important field of SMA application is in medicine, where the pseudo-elasticity is mainly exploited for the realization of several components such as cardiovascular stent, embolic protection filters, orthopedic components, orthodontic wires, micro surgical and endoscopic devices (Chen et all. 2005).

From the microstructural point of view, shape memory and pseudo-elastic effects are due to a reversible solid state microstructural transition from austenite to martensite, which can be activated by mechanical and/or thermal loads as Liu et all. (2000).

Copper-based shape-memory alloys are very sensitive to thermal effects, and it is possible that duringthermal cycles their properties change (e.g., shape-recovery ratio, transformation temperatures, crystal structures, hysteresis and mechanical behavior).

Cu–Zn–Al shape memory alloys exhibit shape memory behavior in a range of composition. It is characterized by a stable high temperature and by a disordered bcc structure named β-phase. After a customized cooling process, a B2 structure is obtained, following a DO3 ordering. It is also know that martensite stabilization can be reduced by a step-quenched treatment.

Cu ZnAl alloys mechanical properties are influenced by (Ameodo et all. 2003):

- martensite stabilization;
- grain size;
- processes procedure (e.g., temperature, heat treatment cycles number).

Other investigations carried out on CuZnAl alloys, showed the deformation influence on the macroscopic behavior and on martensite morphology. Martensitic transformation occurs initially in deformed material and the manufact shape follows the transformation as Kayali et all. (2000). Larger grains dimensions allow an easier transformation process, allowing the growth of 18R martensite (Zhang et all. 1999).

In this work, damaging micromechanism during a tensile test in a CuZnAl alloy has been investigated, focusing the crack initiation and its stable growth. Deformation influence on alloy microstructure has been investigated during the tensile test by means of a X-Ray diffraction**.**

2. Material and methods

In this work a CuZnAl pseudo-elastic alloy, made in laboratory by using controlled atmosphere furnace and characterized by chemical composition shown in table 1, has been used to investigate mechanical behavior in tensile conditions.

The evolution of the microstructure during uniaxial deformation was analyzed by a miniature testing machine which allows in-situ scanning electron microscopic (SEM) observations as well as X-Ray micro-diffraction analyses.

In particular, the testing machine is equipped with a simple and removable loading frame, which allows SEM and

X-Ray analyses at fixed values of applied load and/or deformations. The machine is powered by a stepping motor, which applies the mechanical deformation to the specimen through a calibrated screw, with pitch of 0.8mm, and a control electronic allows simultaneous measurement and/or control of applied load and stroke of the specimen head.

Table 1. Chemical composition of CuZnAl investigated alloy

Cu	Zn	Al	Other
73.00	21.80	5.04	0.16

The stroke is measured by a Linear Variable Differential Transformer (LVDT) while the load is measured by two miniaturized load cells with maximum capacity of 10 kN. Miniature dog bone shaped specimens were machined from alloy samples obtained by cold cutting of mini sheets from as cast ingots, by wire electro discharge machining.

Step by step isothermal tensile tests were carried out, at room temperature, at increasing values of specimens elongation. For each loading step, the loading frame containing the specimen was removed from the testing machine, at fixed values of deformation. The specimens, under load condition, was analyzed by means of:

- a light optical microscope, characterized by a wide observation field; all the investigated specimen length was observed in order to identify the crack initiation site. The investigated steps are ε_{eng} = 0%, 5%, 10%, and 14% (failure);
- a diffractometer in order to evaluate XRD spectra. XRD measurements were made with a Philips X-PERT diffractometer equipped with a vertical Bragg–Brentano powder goniometer. A step–scan mode was used in the 2θ range from 40° to 90° with a step width of 0.02° and a counting time of 2 s per step. The employed radiation was monochromated CuKα (40 kV – 40 mA). The calculation of theoretical diffractograms and the generation of structure models were performed using the PowderCell software (PowderCell 2.3). The investigated steps are at ε_{eng} = 0% and 5%.

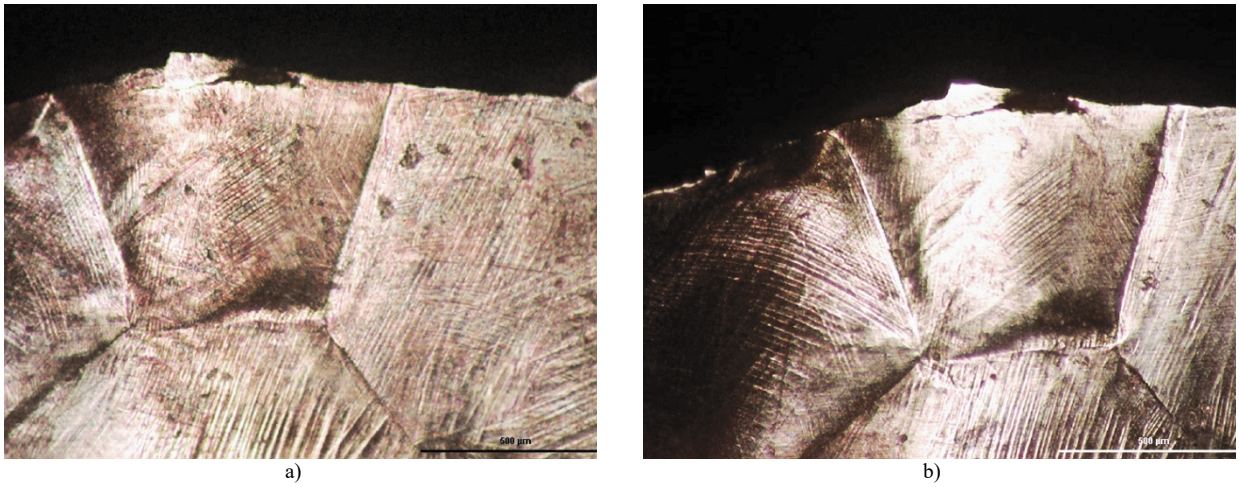

a) b)

Fig. 1. Etched surface: a) etched-deformed and observed, b) deformed, cleaned and re-etched.

Finally, SEM observations on fracture surface have been performed in order to evaluate the main fracture micromechanisms.

In order to check the correctness of the LOM observation procedure, a preliminary test has been performed. An unloaded and metallographically prepared specimen has been deformed up to ε_{eng}=0% and then LOM observed

(figure 1a). Subsequently the same specimen (loaded) has been metallographically prepared and LOM observed (figure 1b). It is evident the possibility to follow the grains modifications in the investigated SMA only performing the first metallographic preparation.

3. Results and discussion

The inhomogeneities of material has been highlighted by crono-amperometric tests which results are shown in figure 2. The electrochemical behaviour is characterized by a decrease of current due to a slight passive property, due to presence of corrosion product formation on the etched surface. But the corrosion products are not homogenous, because the structure appears different between bulk of grains, boundary and a not negligible zone riding on the boundary of grains.

Engineering stress strain curve of investigated alloy is shown in figure 2, where a plateau has not been observed. The investigated deformation conditions correspond to:

- ε_{eng} = 0% - starting test conditions;
- ε_{eng} = 5% - near yield point;
- ε_{eng} = 10% - plastic zone;
- ε_{eng} = 14% - specimen failure.

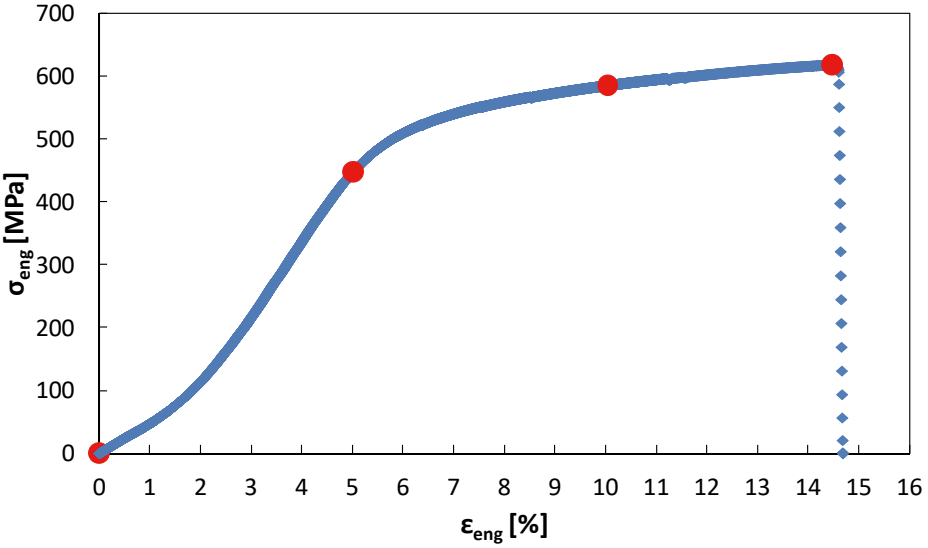

Fig.2. Engineering Stress-Strain curve (red points correspond to the investigated conditions).

The failure initiation site (figure 3), for ε_{eng} = 0%, is characterized by the presence of three grains (figure 3a). For ε_{eng} = 5% (figure 3b) the three grains show an unchanged orientation, no sub-grains nucleation and a grain boundary deformation from linear to curved shape, probably due to phase transition. This is more evident in the grain on the left, where a surface modification is observed (sort of zig-zag lines on the surface).

For ε_{eng} = 10% (figure 3c), an intergranular crack initiate from the lateral specimen surface, with a secondary intergranular crack, that is more or less parallel to the applied load. This secondary crack is probably due to the phases transition in grains with different orientations, with a consequent τ stress increase at the grain boundary as Zhang et all. (1999).

The increase of the macroscopical deformation implies an increase of the localized damage level, with the coalescence of main and secondary cracks (figure 3d). Final failure is obtained by means of a crack propagation

from one side to the opposite side of the specimen ("fracture ending zone").

In figure 4, the "fracture ending zone" is shown. For ε_{eng} = 0, 5 and 10%, corresponding respectively to figure 4a, b and c, no transformations are evident: surface modifications due to phase transformations are not observed in this zone. For ε_{eng} = 14% (figure 4d), it is possible to observe a localized ductile deformation.

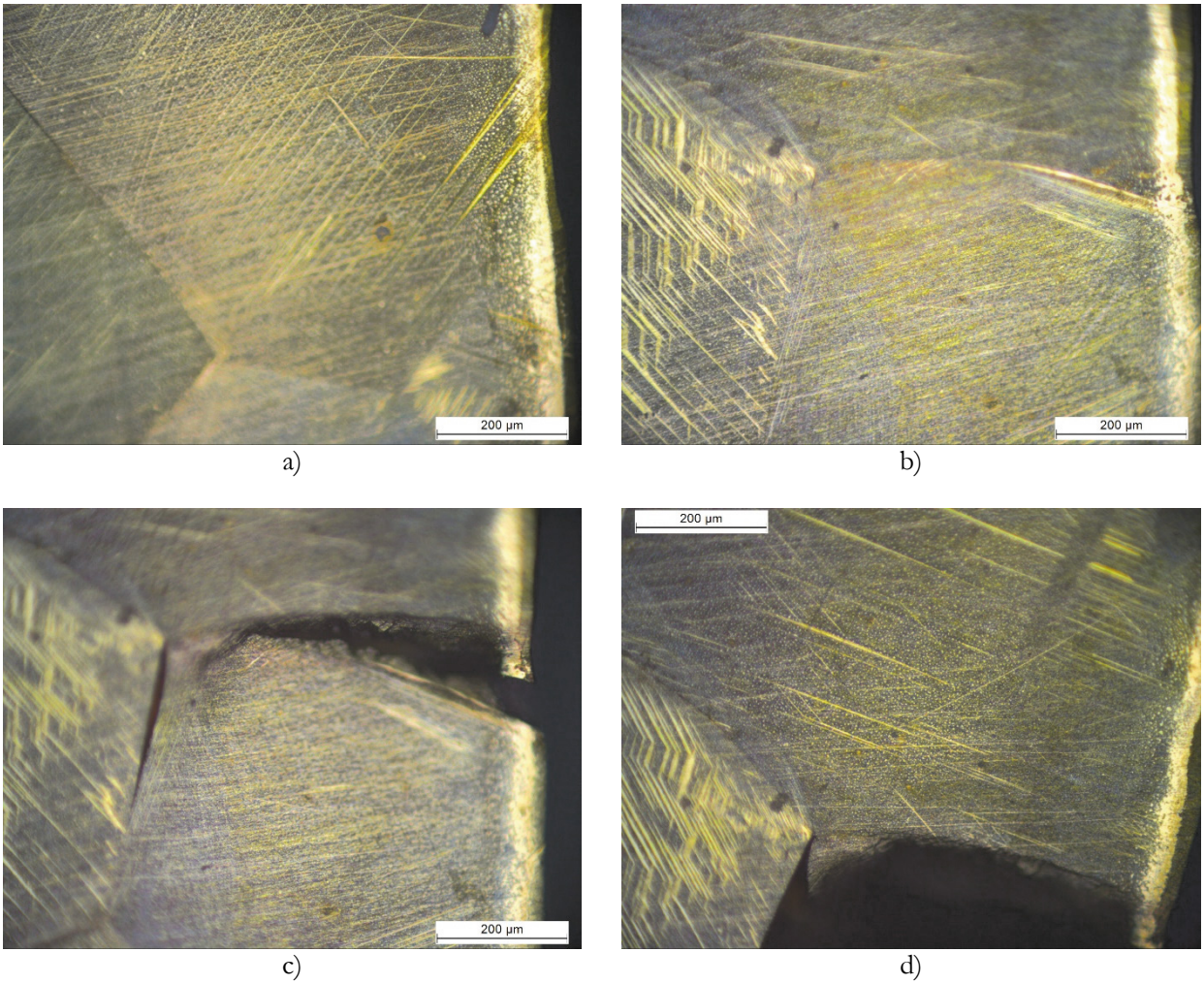

Fig.3. Fracture initiation zone: a) ε_{eng} = 0%, b) ε_{eng} = 5%, c) ε_{eng} = 10%, d) ε_{eng} = 14% (failure).

Evidence of structure transitions are in figure 5, where two diffractograms show respectively the undeformed and the deformed at ε_{eng} = 5% specimen. The undeformed specimen spectrum shows four peaks corresponding to 42.35°, 43.71°, 70.39°, 80.23°. The ε_{eng} = 5% deformed specimen shows also four peaks but corresponding to different diffraction angles (42.27°, 43.43°, 43.85° and 85.71°). Peaks modifications (considering both angles and intensity) show the mechanical deformation influence on the microstructure modifications.

Fracture surfaces are characterized by a brittle morphology, as the intergranular cleavage shown in figure 6a, which confirms the path observed on the lateral surface (figure 3c and d). According to the LOM damaging micromechanisms analysis and to SEM fracture surface analysis, grains decohesion seems to be main damaging micromechamisms.

Inclusions presence implies the initiation of secondary microcracks (figure 6b), probably due to the same mechanism which characterizes the grains decohesion.

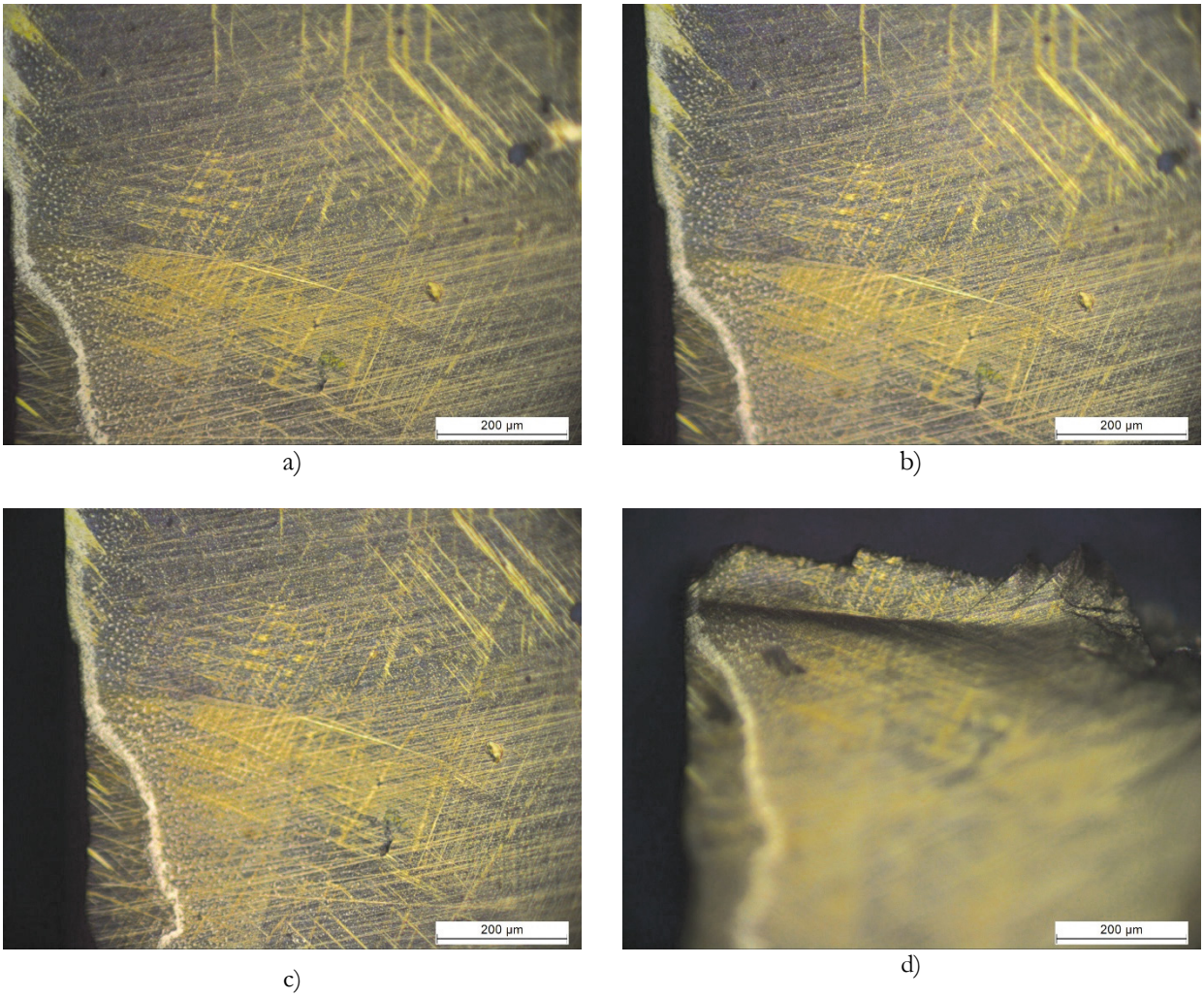

Fig.4. Fracture ending zone: a) ε_{eng} = 0%, b) ε_{eng} = 5%, c) ε_{eng} = 10%, d) ε_{eng} = 14% (failure).

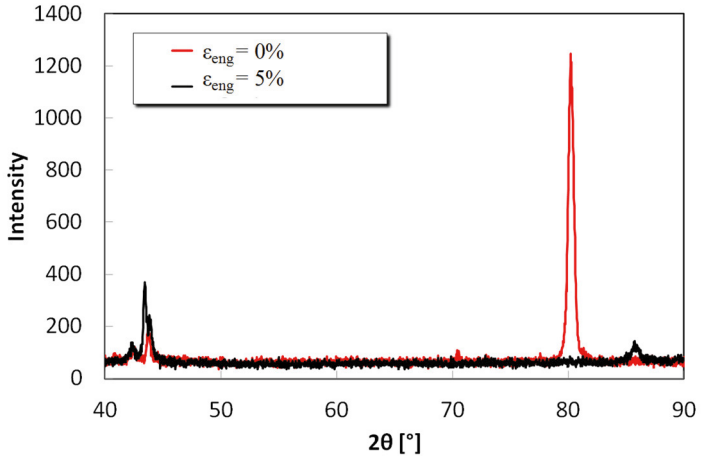

Fig.5. Diffraction spectra.

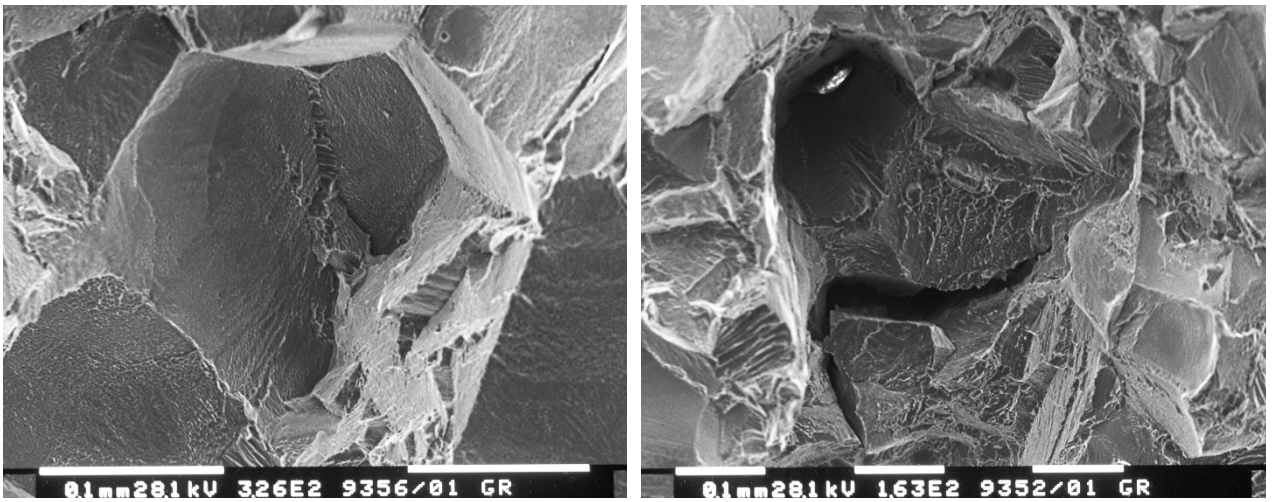

a) b)

Fig.6. Fracture surface: a) intergranular cleavage, b) secondary crack in presence of inclusion.

4. Conclusions

In this work, the main crack initiation and propagation micromechanisms during tensile tests performed on a CuZnAl SMA has been analyzed.

Material has been previously analyzed and characterized in terms of as cast microstructure and in terms of microstructure transition. The evidences of transitions have been investigated by means an X-ray diffraction analyses. According to the experimental results, the following conclusions can be summarized:

- Cracks initiate at grains boundaries due both to high deformation values and to phases transitions;
- Memory effect is not only due to phases transitions, but also to the unchanging of numbers of grains boundary;
- The main fracture surface morphology is brittle and is characterized by intergranular cleavage.

Results of analyses show the influence of boundary grains inhomogeneity on the crack micromechanisms due to different local chemical composition. In the other hands, the shape memory performances of CuZnAl alloys could be improved using processes and/or techniques which allows to homogenize the microstructure of material.

A better homogeneity of grains, may also improves the ductility of materials, because the main fracture micromechanism observed by means of SEM, is a brittle intergranular crack propagation.

References

Arneodo Larochette, P., Ahlers, M., 2003. Grain-size dependence of the two-way shape memory effect obtained by stabilisation in Cu–Zn–Al crystals, Materials Science and Engineering. A361, 249–257

Chen, B., Liang, C., Fu, D., 2005. Pitting Corrosion of Cu-Zn-Al Shape Memory Alloy in Simulated Uterine Fluid, J. Mater. Sci. Technology, 21(2), 226-230.

Dong, Y., Boming, Z., Jun, L., 2008. A Changeable Aerofoil Actuated by Shape Memory Alloy Springs, Materials Science and Engineering A, 485, 243–250.

Kayali, N., Ozgen, S., Adiguzel, O., 2000. Strain effects on the macroscopic behaviour and martensite morphology in shape-memory CuZnAl alloys, Journal of Materials Processing Technology. 101, 245-249.

Liu, Y., Tan, G.S., 2000. Formation of interfacial voids in cast and micro-grained γ′-Ni3Al during high temperature oxidation, Intermetallics 8, 1385-1391.

Otsuka, K., Ren, X., 2005. Physical metallurgy of Ti–Ni-based shape memory alloys, Progress in Materials Science 511.

PowderCell 2.3—Pulverdiffraktogramme aus Einkristalldaten und Anpassung experimenteller Beugungsaufnahmen, in http://www.bam.de/de/service/publikationen/powder_cell.htm.

Zhang, J.X., Zheng, Y.F., Zhao, L.C., 1999. The Structure and Mobility of Intervariant Boundaries in 18R Martensite in a Cu-Zn-Al Alloy, Acta mater. 47(7), 2125-2141.